

Absence of the blood-clotting regulator thrombomodulin causes embryonic lethality in mice before development of a functional cardiovascular system

(gene targeting/embryonic growth retardation)

AILEEN M. HEALY, HELEN B. RAYBURN, ROBERT D. ROSENBERG*, AND HARTMUT WEILER

Department of Biology, Massachusetts Institute of Technology, Cambridge, MA 02139

Communicated by David E. Housman, Massachusetts Institute of Technology, Cambridge, MA, October 18, 1994

ABSTRACT We have targeted the murine thrombomodulin (TM) gene in embryonic stem cells and generated embryos as well as mice with TM deficiency. The heterozygous TM-deficient (TM⁺/-) mice as compared to wild-type (TM⁺/+) littermates exhibit 50% reductions in the levels of TM mRNA and TM protein. However, TM⁺/- mice appear normal and are free of thrombotic complications. The homozygous TM-deficient (TM⁻/-) embryos die before embryonic day 9.5. An overall retardation in growth and development of TM⁻/- embryos is first evident on embryonic day 8.5 (8–12 somite pairs). However, no specific pathologic abnormalities are observed. These initial changes take place at a time when TM is normally expressed in the parietal yolk sac. The removal of embryonic day 7.5 TM⁻/- embryos from maternal decidua and their subsequent culture *in vitro* allow development to proceed to stages not observed *in vivo* (13–20 somite pairs) with the appearance of normal blood vessels in the visceral yolk sac and embryo. The results of our studies suggest that the failure of TM⁻/- embryos to survive at mid-gestation is a consequence of dysfunctional maternal-embryonic interactions caused by the absence of TM in the parietal yolk sac and demonstrate that the receptor is necessary for normal embryonic development *in utero*.

Thrombomodulin (TM) is a natural anticoagulant that forms a 1:1 complex with thrombin (1). This interaction product converts protein C (PC) to its activated form (APC), which proteolytically destroys activated cofactors V and VIII and thereby suppresses generation of thrombin. TM is expressed on vascular endothelial cells and also on synovial cells, meningeal cells, mononuclear phagocytes, and platelets (1, 2). TM has also been detected in the rodent embryo on the parietal endoderm of yolk sac, in the aortic arch, embryonic heart, blood vessels, lung buds, and in the developing central nervous system (3, 4). The widespread distribution of TM in embryos and adult animals suggests that the receptor may have alternative functions beyond anticoagulation.

In the present investigation, we have targeted the intronless TM gene in embryonic stem (ES) cells and generated mice that transmit the receptor deletion to their progeny. The results demonstrate that mice heterozygous for the TM deletion exhibit half-normal levels of receptor and should serve as a model for defining the contributions of TM to thrombogenesis. The data also show that embryos homozygous for the TM deletion die *in utero* by embryonic day 9.5 (E9.5) and suggest this lethal phenotype is due to an overall growth retardation secondary to a defect in the parietal yolk sac.

MATERIALS AND METHODS

Targeting the TM Gene in ES Cells and Generation of TM-Deficient Mice. The D3 ES cells (provided by R. Hynes, Massachusetts Institute of Technology) were electroporated with a *Not* I-linearized targeting vector (see Fig. 1A) and selected in growth medium containing G418 and gancyclovir (gift of Syntex, Palo Alto, CA); doubly resistant colonies were isolated as described (5). The correctly targeted ES clones were identified and used to generate chimeric animals by injection into host blastocysts.

Quantification of TM mRNA and Protein Levels. The relative levels of TM mRNA were determined by RNase protection assays. The TM cRNA probe was obtained by subcloning a *Pst* I fragment of mouse TM cDNA (nucleotides 674–972) into pBluescript II (Stratagene) and transcribing the *Pvu* II-cut plasmid with T7/3 polymerase. RNA was hybridized simultaneously with ³²P-labeled TM and β-actin cRNA (pTRI-actin, Ambion, Austin, TX) and digested with RNase A/T1; protected fragments were resolved by electrophoresis and quantified.

Lung fragments were labeled *ex vivo* with 1 mCi of [³⁵S]methionine per ml (1 Ci = 37 GBq; Trans³⁵S-label, ICN). The radiolabeled tissue was homogenized and immunoprecipitated with rat anti-mouse TM monoclonal antibody (mAb) 273-34A (gift of S. Kennel, Oak Ridge National Labs, Oak Ridge, TN) as described (6). The immunoprecipitates were collected on protein G-Sepharose (Pharmacia) and bound proteins eluted with SDS buffer were electrophoresed under reducing conditions. ³⁵S-labeled TM-specific bands were excised from dried gels and quantified.

The steady-state levels of TM protein in whole tissue extracts were measured by a two-site, solid-phase radioimmunoassay with mAb 273-34A and 201B as outlined (7). The determination of TM-dependent activation of PC by thrombin on isolated mouse thoracic aortic segments was performed as described (8). For analysis of TM cofactor activity, TM was immunocaptured from lung as outlined above and then quantified as described for vessel segments.

Histology. Embryos obtained from timed matings were dissected from uteri, fixed, and either stained with hematoxylin/eosin or genotyped as described (5).

Whole Embryo Culture. Presomite stage TM^{+/+}, TM^{+/-}, and TM^{-/-} embryos (E7.5–E8.0) were dissected free of maternal tissue, Reichert's membrane was removed, and embryos were transferred to Dulbecco's modified Eagle medium supplemented with 50% rat serum and cultured for 48 hr as described (9).

The publication costs of this article were defrayed in part by page charge payment. This article must therefore be hereby marked "advertisement" in accordance with 18 U.S.C. §1734 solely to indicate this fact.

Abbreviations: TM, thrombomodulin; ES, embryonic stem; E, embryonic day; mAb, monoclonal antibody(ies); PC, protein C; APC, activated PC.

*To whom reprint requests should be addressed at: Massachusetts Institute of Technology, 77 Massachusetts Avenue 68-480, Cambridge, MA 02139.

RESULTS

TM Gene Disruption in ES Cells and Generation of TM Chimeric Mice. We cloned a 17-kb TM gene fragment from a genomic library of the 129 Sv mouse. This clone spans the entire mRNA coding domain as well as 9 kb and 5 kb of 5' and 3' flanking regions, respectively. The 129 Sv mouse and D3 ES cell TM genes exhibit an intracisternal A particle (IAP)-like element inserted 2462 bp upstream of the mRNA coding region as described for the 129/J mouse TM gene (10).

We then constructed a replacement-type targeting vector (Fig. 1A) containing about 8 kb of genomic TM sequence

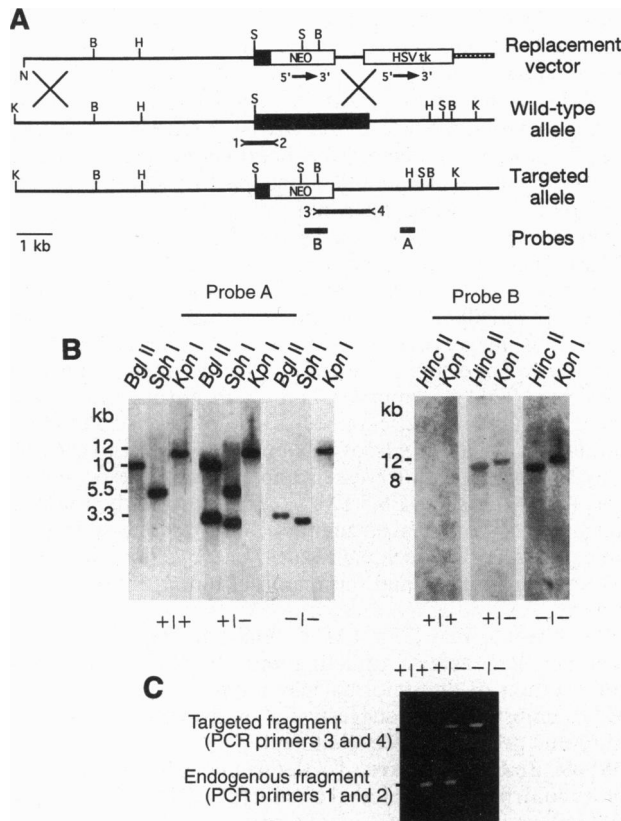


FIG. 1. Scheme for targeting the intronless TM gene and analysis of targeted cells and mutant mice. (A) The TM replacement vector was constructed by inserting a *Sal* I, *Sph* I TM gene fragment containing 6.8 kb of 5' upstream sequence including the transcriptional start site and 153 bp of 5' untranslated TM sequence into a unique *Xho* I site of the plasmid pPNT. The neo expression cassette is followed by an 896-bp TM gene fragment corresponding to 3' untranslated TM mRNA sequence (nucleotides 2747–3643, GenBank accession no. X14432) and the thymidine kinase (tk) gene (11). HSV, herpes simplex virus. The neo expression cassette replaces the TM coding region (closed box) plus 860 bp of 3' flanking sequence. Probe A is a 300-bp *Xba* I–*Bam*HI TM fragment hybridizing to sequences 500 bp downstream of the targeting construct. Probe B is a 640-bp *Pst* I fragment of the neo gene. PCR primers and amplified regions are indicated as numbered bars, 1–2 and 3–4. PCR primer 1 is 5'-AGGTTGTGATA-GAGGCTAGCTGCTGTC-3' and primer 2 is 5'-GTGTTGATAGG-TACTAGAGATGTGGCA-3'. PCR primer 3 is 5'-CTATCGCCT-TCTTGACGAGTCTCTCTG-3' in the neo gene and primer 4 is 5'-CAGCCTGTAATGTATCTCTCTGAAG-3' located 3.8 kb downstream of the TM transcription initiation site. Restriction enzyme sites indicated are *Bgl* II (B), *Hinc*II (H), *Kpn* I (K), and *Sph* I (S). (B) Southern blot analysis of genomic DNA from wild-type (+/+), heterozygotes (+/-), and TM null mutants (-/-). (C) PCR primers 1 and 2 were employed to identify a 770-bp fragment present only within the endogenous TM gene (-35 bp to +735 bp relative to transcription initiation). PCR primers 3 and 4 were utilized to detect a 1.5-kb fragment present only in the targeted allele. The ethidium bromide-stained fragments show the expected pattern from TM^{+/+}, TM^{+/-}, and TM^{-/-} genomic DNA.

including IAP-like retroviral sequences. In two separate experiments, 3.25×10^8 ES cells were transfected with the TM targeting vector and 648 doubly drug-resistant clones were analyzed by Southern analyses. Southern blot analysis with probes A and B (Fig. 1A) revealed the expected ratio of the endogenous versus the targeted gene fragments, the predicted pattern of hydrolysis at sites internal to (*Bgl* II and *Sph* I) and external to (*Kpn* I) the insertion site, and a single integration site (Fig. 1B). These results, in conjunction with PCR analysis (Fig. 1C), confirm the correct replacement of the TM gene in the targeted ES cell clones.

The above analyses identified 4 of 648 doubly drug-resistant ES cell clones that exhibited the pattern described above. The 4 clones were employed to generate chimeric C57BL/6J mice, but only 2 clones (C14-15 and D5-11) derived from independent transfections transmitted the targeted TM allele to their progeny.

Characterization of TM^{+/-} Mice. We next determined the levels of TM mRNA and TM protein in 10- to 12-week-old male mice. The levels of TM mRNA were quantified by RNase protection assays for lung, spleen, heart, kidney, and brain. In all tissues, the abundance of TM mRNA relative to β -actin mRNA in four sibling pairs of TM^{+/-} mice as compared to TM^{+/+} littermates is reduced to $57\% \pm 8\%$ ($n = 4$). The extent of *de novo* biosynthesis of TM protein was measured by *ex vivo* metabolic labeling of lung fragments and subsequent quantification of radiolabeled receptor. The TM-specific cpm in equivalent amounts of lung extract in three sibling pairs of TM^{+/-} mice as compared to TM^{+/+} littermates is decreased to 57% (111 ± 10 cpm versus 194 ± 13 cpm, $n = 3$). The steady-state concentration of TM protein in organ extracts was ascertained with a solid-phase, double antibody radioimmunoassay. The level of TM protein in equivalent amounts of extract from lung in four sibling pairs of TM^{+/-} mice as compared to TM^{+/+} littermates is reduced to 49% [894 ± 200 ¹²⁵I-labeled mAb (¹²⁵I-mAb) cpm/ μ g of tissue protein versus 1820 ± 279 ¹²⁵I-mAb cpm/ μ g of tissue protein, $n = 4$] and 53% in spleen (26.8 ± 2.5 ¹²⁵I-mAb cpm/ μ g of tissue protein versus 50.3 ± 3.8 ¹²⁵I-mAb cpm/ μ g of tissue protein, $n = 4$). Finally, TM cofactor activity in lung extracts or on thoracic aortic segments was also determined. The level of TM cofactor activity in lung extracts in two sibling pairs of TM^{+/-} mice as compared to TM^{+/+} littermates and on thoracic aorta segments of known size in three sibling pairs of TM^{+/-} mice as compared to TM^{+/+} littermates is decreased to 53% (2.51 ± 0.40 ng of APC generated per min versus 4.66 ± 0.56 ng of APC generated per min, $n = 6$) and 49% (0.12 ± 0.04 ng of APC generated per min versus 0.24 ± 0.04 ng of APC generated per min, $n = 6$), respectively.

Despite a 50% reduction in the levels of TM, TM^{+/-} mice are healthy, normal in size as well as weight, and fertile. The TM^{+/-} mice, now >1 year old, display no gross abnormalities. Histologic analyses of lung, brain, kidney, heart, liver, and spleen from TM^{+/-} mice as compared to TM^{+/+} littermates reveal no pathologic abnormalities including the absence of thrombi (not shown).

Homozygous Deletion of the TM Gene Leads to an Embryonic Lethal Mutation. We then interbred TM^{+/-} mice to generate TM^{-/-} animals. Progeny derived from ES cell clone C14-15 were mated and produced 99 offspring. Thirty-five of these progeny are TM^{+/+} and 64 are TM^{+/-}, while no TM^{-/-} mice were born. Progeny derived from ES clone D5-11 were bred and generated 53 offspring. Twenty-one of the progeny are TM^{+/+} and 32 are TM^{+/-}; again no TM^{-/-} mice were born. These results suggest that the homozygous TM deletion is an embryonic lethal mutation.

To determine when the homozygous TM deletion leads to embryonic lethality, we interbred TM^{+/-} mice, isolated em-

Table 1. Progeny from TM^{+/-} interbreeding

Stage	No. of litters	Total progeny	Genotype		
			+/+	+/-	-/-
E7.5	3	27	11	12	4
E8.5	8	59	21	27	11
E9.5	3	20	3	13	4*
E10.5	9	61	24	37	0
E12.5	1	10	3	7	0
E16.5	1	7	5	2	0
E17.5	1	3	2	1	0
E18.5	1	5	2	3	0
P28	32	152	56	96	0

Genotypes of embryos are the sum of intercrosses of progeny derived from clone C14-15 and intercrosses between progeny derived from clones C14-15 and D5-11. Genotypes of adult mice (P28) are the sum of intercrosses of progeny derived from clone C14-15 in addition to intercrosses of progeny derived from clone D5-11.

*Embryos are grossly abnormal.

bryos at different gestation times, and then examined whole mounts as well as genotyped embryos (Table 1). TM^{-/-} embryos are present up to E9.5, but not at later time points. The results were generated by intercrossing progeny derived from ES cell clone C14-15, with the exception of E8.5 and E10.5, which were produced by intercrossing progeny derived from ES cell clone C14-15 as well as intercrossing progeny derived from C14-15 with progeny derived from clone D5-11. The identical results obtained for the various matings on each of these 2 days indicate that the absence of TM^{-/-} embryos at E10.5 and beyond is due to the effect of the targeted allele rather than a secondary mutation in ES cells.

Analyses of whole-mount embryos reveal that E7.5 TM^{-/-} embryos as compared to TM^{+/+} and TM^{+/-} littermates appear normal in size, the prospective head folds and neural grooves are prominent (Fig. 2, compare *A*, *D*, and *G*), and the primitive streaks and extraembryonic cavities are evident. Similar examination of E8.5 TM^{+/+}, TM^{+/-}, and TM^{-/-} embryos reveals prominent somites (6–12 pairs) (Fig. 2 *B*, *E*, and *H*), neural tube closure in the mid-somitic region (not shown), and clearly formed head folds. Although this stage of development is characterized by a wide intralitter variation in size and maturity, E8.5 TM^{-/-} embryos are consistently among the smallest and least developed of their litters. By E9.5, TM^{-/-} embryos are severely abnormal when compared to their TM^{+/+} and TM^{+/-} littermates, showing no discernible embryonic landmarks (Fig. 2, compare *I* with *C* and *F*).

Sagittal sections through E8.5 embryos show intact, well-formed TM^{-/-} embryos, which are always among the smallest and least developed within their litter (Fig. 3, compare *A* with *B*). Within the embryonic tissues, TM^{-/-} embryos customarily reveal a normal cephalic region and a normal head mesenchyme. However, the cephalic volume of TM^{-/-} embryos is significantly smaller than that of TM^{+/+} and TM^{+/-} littermates. The somites and neural tube also appear normal (not shown in Fig. 3*B*). As represented in Fig. 3*A*, TM^{+/-} embryos possess a heart with two clearly formed chambers surrounded by a myocardium, and lined by an endocardium. The embryonic heart contains nucleated red blood cells, which indicates fusion of the extraembryonic, visceral yolk sac vasculature with the embryonic vasculature and the initial contractions of the heart to allow circulation of blood cells. As represented in Fig. 3*B*, TM^{-/-} embryos typically possess a heart with a single chamber surrounded by a myocardium but have yet to develop an endocardium. The embryonic heart contains no nucleated red blood cells, which implies that the extraembryonic and embryonic vasculature have not yet undergone fusion and cardiac contractions have not been initiated.

The extraembryonic membranes of E8.5 TM^{-/-} embryos as compared to normal littermates are identical, the amnion is intact, and the allantois is extending toward or fused with the chorion. In all genotypes, we note a continuous Reichert's membrane lined by a morphologically normal parietal endoderm. TM^{-/-} embryos and their normal littermates exhibit a well-formed visceral yolk sac. The visceral endoderm contains an extensive microvillus border apposed to the yolk cavity and blood islands/vessels apposed to the exocoelomic cavity (Fig. 4). Finally, E8.5 TM^{-/-} embryos and their normal littermates elaborate a normal-appearing trophectoderm as well as surrounding decidual tissues. There is no evidence of leukocyte infiltration and the maternal blood sinuses appear similar.

We conclude that E7.5 TM^{-/-} embryos have no obvious developmental defects affecting morphogenesis. The first manifestation of an abnormal phenotype is evident in E8.5 TM^{-/-} embryos and is suggestive of an overall retardation of embryonic growth and development.

Whole Embryo Culture. To determine whether maternal factors contribute to the lethal phenotype of TM^{-/-} embryos, we employed an *in vitro* whole embryo culture system to compare the development of TM^{+/+}, TM^{+/-}, and TM^{-/-} littermates from E7.5 through E9.5. We isolated 47 E7.5 embryos from nine litters and studied their development *in vitro* over the next 48 hr (Table 2). We observe that develop-

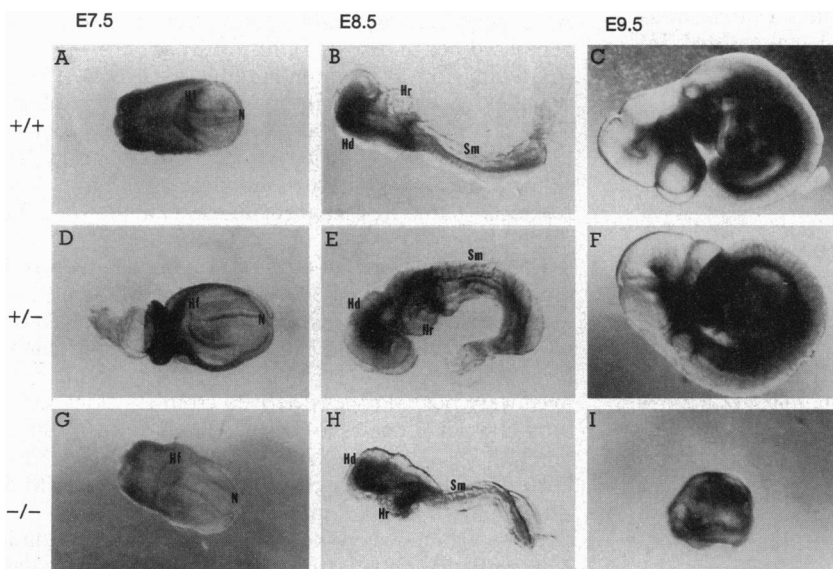


FIG. 2. Whole-mount photomicrographs of TM^{+/+}, TM^{+/-}, and TM^{-/-} embryos at E7.5, E8.5, and E9.5. Hd, head; Hr, prospective head fold; Hr, heart; Sm, somites; N, neural groove. (E7.5 \times 30, E8.5 \times 25, E9.5 \times 20.)

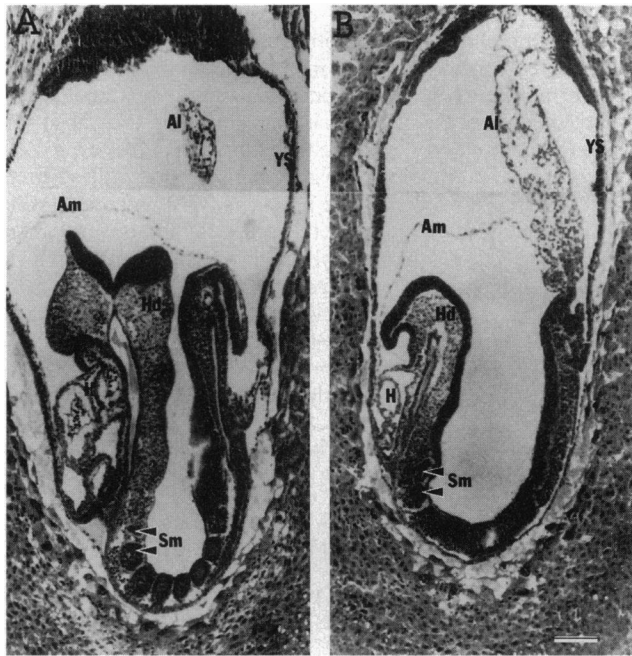


FIG. 3. Histologic analyses of $TM^{+/-}$ and $TM^{-/-}$ embryos indicate an overall growth retardation. Representative images of sagittal sections through E8.5 $TM^{+/-}$ (A) and $TM^{-/-}$ (B) embryos stained with hematoxylin/eosin. Al, allantois; Am, amnion; Hd, head; Hr, heart; Sm, somites; YS, yolk sac. (Bar = 500 μ m.)

ment of the 40 $TM^{+/+}$ and $TM^{+/-}$ embryos is slightly retarded *in vitro* as compared to *in vivo* as described for whole embryo culture (12). However, all 7 $TM^{-/-}$ embryos progress *in vitro* to a developmental stage not observed *in vivo* (up to 20 somites, a vascular network in the visceral yolk sac, and a rapidly beating heart) and are identical in size to $TM^{+/+}$ and $TM^{+/-}$ littermates of the same developmental stage. These observations indicate that the maternal decidual environment contributes significantly to the embryonic lethal phenotype in $TM^{-/-}$ embryos. However, none of the $TM^{-/-}$ embryos attains the most advanced *in vitro* developmental stage observed for $TM^{+/+}$ and $TM^{+/-}$ embryos, which suggest that maternal factors may have already affected E7.5 $TM^{-/-}$ embryos prior to isolation or that a second block in development of the $TM^{-/-}$ embryos has been revealed.

DISCUSSION

We deleted by homologous recombination one of two *TM* genes in ES cells and generated chimeric mice that transmitted

Table 2. *In vitro* whole embryo culture

Genotype	No. of embryos	Somite pairs		Beating heart	Fused vasc.*	Axial rotation
		13–20	21–29			
$TM^{+/+}$	20	16	4	20	10	2
$TM^{+/-}$	20	16	4	20	7	2
$TM^{-/-}$	7	7	0	7	0	0

*Fusion of the vasculature is determined by the presence of circulating blood cells within the visceral yolk sac.

the mutant allele to their progeny. The resultant $TM^{+/-}$ animals as compared to $TM^{+/+}$ littermates exhibit 50% reductions in the concentrations of *TM* mRNA and *TM* protein. However, $TM^{+/-}$ mice fail to exhibit a thrombotic phenotype. It is of interest that heterozygous mutations of the *PC-TM* pathway are quite common in humans (13, 14), but expression of the thrombotic phenotype in affected individuals is augmented by only about 5- to 10-fold as compared to the general population (15). This suggests that humans with a heterozygous deficiency of the *PC-TM* pathway exhibit a hypercoagulable state that sensitizes them to a second genetic defect, which leads to the eventual development of a thrombotic event. As additional animals become available with other genetic defects in the hemostatic mechanism, it will be possible to test whether it is a combination of mutations in the coagulation pathway that leads to the development of thrombotic events.

Our most interesting finding is that $TM^{-/-}$ embryos die and are resorbed by E10.5. The examination of whole mounts and histologic sections reveals that E7.5 $TM^{-/-}$ embryos are identical in size to normal littermates, whereas E8.5 $TM^{-/-}$ embryos are smaller and less well developed but have no specific abnormalities of organogenesis as compared to normal littermates. Within 24 h, the $TM^{-/-}$ embryos have undergone complete degeneration. These observations suggest that the loss of *TM* function exerts a profoundly negative effect on the overall growth and development of embryos between E7.5 and E8.5.

Given that *TM* is an integral membrane protein, we presume that the receptor functions at its site of synthesis. Immunohistochemical investigations demonstrate that *TM* is expressed at E7.5 in parietal endoderm and then synthesized at E9.5 in other organ systems (4). Therefore, the earliest morphologic abnormalities detected in $TM^{-/-}$ embryos are concurrent with receptor expression in the parietal yolk sac and immediately precede *TM* expression in other organ systems.

As described above, the *in vivo* development of $TM^{-/-}$ embryos is halted at E8.5. The *in vitro* culture of E7.5 $TM^{-/-}$ embryos allows their progression to proceed to a later devel-

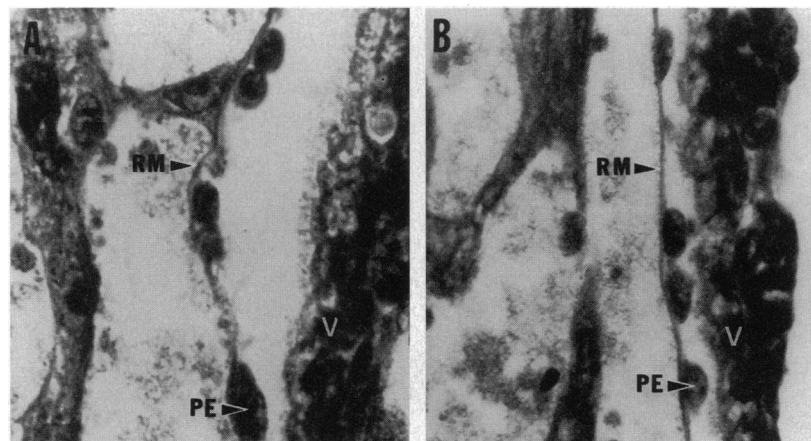


FIG. 4. Histologic analyses of $TM^{+/-}$ and $TM^{-/-}$ yolk sacs reveal normal structures. High-power view of the yolk sac shown in Fig. 3 from E8.5 $TM^{+/-}$ (A) and E8.5 $TM^{-/-}$ (B) embryos. RM, Reichert's membrane; PE, parietal endoderm cells; V, visceral endoderm. ($\times 680$.)

opmental stage in which embryos display an extensive, anastomotic plexus of blood vessels in the visceral yolk sac and a well-developed, regularly contracting heart. Thus, the removal of the TM^{-/-} embryos from the maternal decidua permits formation of structures not observed *in utero*. These results support the hypothesis that the intrinsic defect in the TM^{-/-} embryo leads to virtually complete inhibition of growth and development between E7.5 and E8.5 because of dysfunctional maternal-embryonic interactions.

The parietal yolk sac, the outermost of extraembryonic membranes, is permeable to macromolecules intravenously injected into the maternal circulation (16) and presumably functions as a permeability barrier during gastrulation and early somitogenesis. Disruption of the components of the parietal yolk sac (trophoblast cells, Reichert's membrane, or parietal endoderm) at this critical developmental stage may have severe consequences on embryonic growth and development. Indeed, antibodies directed against semipurified preparations of Reichert's membrane have been injected into pregnant rats on E9.0 (17). The antibodies bound specifically to antigens on Reichert's membrane and caused either fetal resorption (highest doses) or fetal growth retardation (decreasing doses). Although the precise function of these antigens remains unknown, the phenotype observed is similar to that of TM^{-/-} embryos.

The extensive tissue remodeling that occurs prior to placentation at the interface between the embryo and maternal circulation may create a hypercoagulable microenvironment in close proximity to the parietal yolk sac. The generation of thrombin at the above site must occur within the maternal circulation since *in situ* analysis reveals that embryonic prothrombin is not synthesized until E12.5 (18). It is possible that TM expressed in parietal yolk sac functions to suppress production of thrombin. Indeed, Reichert's membrane contains anticoagulatively active heparan sulfate proteoglycans that could inhibit thrombin, and the parietal endoderm secretes tissue-type plasminogen activator (t-PA), which could produce plasmin that lyses fibrin deposited in this region.

The above observations suggest three potential explanations for the death of TM^{-/-} embryos. (i) Increased levels of maternal thrombin may be generated at the maternal-embryonic interface leading to fibrin deposition. We have observed by immunocytochemistry, using a rabbit anti-human fibrinogen antibody, increased amounts of fibrinogen/fibrin surrounding the extraembryonic membranes of TM^{-/-} embryos as compared to TM^{+/+} and TM^{+/-} littermates (not shown). The deposition of fibrin could damage the parietal yolk sac and thereby restrict exchange of macromolecules. However, it will be necessary to develop specific antibodies against fibrin that do not crossreact with fibrinogen to test this hypothesis rigorously. (ii) Fibrin deposition in the vicinity of the parietal yolk sac could facilitate interaction of t-PA with maternal plasminogen, which would result in plasmin generation. This proteolytic enzyme might lyse fibrin deposited in this region but then also degrade components of Reichert's membrane and the parietal endoderm, which are critically involved in their barrier function. Indeed, experimental evidence

obtained from *in vitro* studies shows that laminin present in Reichert's membrane is susceptible to plasmin degradation (19). (iii) Elevated concentrations of maternal thrombin generated at the interface between TM^{-/-} embryos and the maternal circulation could also be involved in signaling via the thrombin receptor. It is of interest that the thrombin receptor is expressed by the embryo several days prior to the appearance of its normal ligand (18). It is possible that the absence of TM on parietal yolk sac allows maternal thrombin to escape inhibition and then prematurely activate the embryonic thrombin receptor, which could then exert a pernicious effect on the developing embryo. In humans, TM is expressed on the syncytiotrophoblast and is therefore also positioned at the maternal-embryonic interface. Thus, our observations on embryonic lethality may have relevance to the mechanisms of early fetal death in humans.

We thank Richard Hynes for a critical reading of the manuscript and Stephen Kennel for anti-TM monoclonal antibodies. This work was supported by National Institutes of Health Grants HL33014 and HL41484. A.M.H. was supported by a research fellowship award from the American Heart Association, Massachusetts Affiliate.

1. Esmon, C. T. (1987) *Science* **235**, 1348-1352.
2. Boffa, M.-C., Burke, B. & Haudenschild, C. C. (1987) *J. Histochem. Cytochem.* **35**, 1267-1276.
3. Imada, S., Yamaguchi, H., Nagumo, N., Katayanagi, S., Iwasaki, H. & Imada, M. (1990) *Dev. Biol.* **140**, 113-122.
4. Ford, V. A., Wilkinson, J. E. & Kennel, S. J. (1993) *Roux's Arch. Dev. Biol.* **202**, 364-370.
5. George, E. L., Georges-Labouesse, E. N., Patel-King, R. S., Rayburn, H. B. & Hynes, R. O. (1993) *Development (Cambridge, U.K.)* **119**, 1079-1091.
6. Tsiang, M., Lentz, S. R., Dittman, W. A., Wen, D., Scarpati, E. M. & Sadler, J. E. (1990) *Biochemistry* **29**, 10602-10612.
7. Kennel, S. J., Lankford, T., Hughes, B. & Hotchkiss, J. A. (1988) *Lab. Invest.* **59**, 692-701.
8. Salem, H. H., Maruyama, I., Ishii, H. & Majerus, P. W. (1984) *J. Biol. Chem.* **259**, 12246-12251.
9. Baldwin, H. S., Lloyd, T. R. & Solursh, M. (1994) *Circ. Res.* **74**, 244-252.
10. Ford, V. A. & Kennel, S. J. (1993) *DNA Cell Biol.* **12**, 311-318.
11. Carmeliet, P., Schoonjans L., Keikens, L., Ream, B., Degen, J., Bronson, R., DeVos, R., van den Oord, J. J., Collen, D. & Mulligan, R. C. (1994) *Nature (London)* **368**, 419-425.
12. Hunter, E. S., Balkan, T. & Sadler, T. W. (1988) *J. Exp. Zool.* **245**, 264-269.
13. Bertina, R. M., Koeleman, B. P. C., Koster, T., Rosendaal, F. R., Dirven, R. J., de Ronde, H., van der Velden, P. A. & Reitsma, P. H. (1994) *Nature (London)* **369**, 64-67.
14. Miletich, J., Sherman, L. & Broze, G. (1987) *N. Engl. J. Med.* **317**, 991-996.
15. Bovill, E. G., Bauer, K. A., Dickerman, J. D., Callas, P. & West, B. (1989) *Blood* **73**, 712-717.
16. King, B. F. (1972) *Am. J. Anat.* **134**, 365-376.
17. Leung, C. C. K. (1977) *J. Exp. Zool.* **200**, 295-302.
18. Soifer, S. J., Peters, K. G., O'Keefe, J. & Coughlin, S. R. (1994) *Am. J. Pathol.* **144**, 60-69.
19. Inoue, S., Leblond, C. P. & Laurie, G. W. (1983) *J. Cell Biol.* **97**, 1524-1537.